Analysis tools for MesonEx at CLAS12

D. I. Glazier

Citation: AIP Conference Proceedings **1735**, 070003 (2016); doi: 10.1063/1.4949451
View online: http://dx.doi.org/10.1063/1.4949451
View Table of Contents: http://scitation.aip.org/content/aip/proceeding/aipcp/1735?ver=pdfcov
Published by the AIP Publishing

Analysis Tools for MesonEx at CLAS12

D.I. Glazier for the CLAS Collaboration[1,a)]

[1]*School of Physics and Astronomy, University of Glasgow*

[a)]Corresponding author: Derek.Glazier@glasgow.ac.uk

Abstract. The JLAB upgrade will soon be completed and the new CLAS12 detector system will collect large volumes of data allowing detailed investigations of many aspects of hadron physics. The focus of the MesonEx experiment is on the production of mesonic states by low Q^2 virtual photons, or quasi-real photons. Studying such mesonic states is a particularly challenging data analysis problem, requiring well understood detector systems, clean signal and background separation, handling of large volumes of data and crucially a close collaboration between experimentalists and theorists to ensure the most sophisticated theoretical methods are used to interrogate the data. Here we briefly outline some of the analysis and methods that are being used to prepare for the MesonEx experiment.

Experiment

CLAS12

The new CLAS12 detector for the upgraded 11 GeV CEBAF electron beam will feature several improvements from the original. The luminosity will be an order of magnitude higher; the forward detector will allow for improved particle identification, including neutrals; a silicon-strip/micromegas hybrid detector will give precise vertex measurements; and a forward electron detector will allow tagging of low Q^2 virtual photons which contribute a high flux of events into the overall detector. This latter component is designed for and crucial to the meson spectroscopy experiment MesonEx.

While these new features extend the capabilities of the spectrometer the fundamental design builds on the highly successful original CLAS detector. The dominant aspect is six superconducting coils producing a non-uniform toroidal magnetic field. Each sector will contain three regions of drift chambers used to track charged particles and reconstruct their momenta; scintillator counters for particle identification based on time of flight; Cerenkov counters to identify electrons; and electromagnetic calorimeters to measure electrons and neutral particles. This will allow precise measurements of particles up to 35° which dominates the production phase space at the desired beam energies. The recoiling nucleons will be captured in a new dedicated central detector consisting of the vertex detector, time-of-flight scintillators and a scintillator barrel for neutron detection.

MesonEx

The goal of the MesonEx experiment is to use the CLAS12 spectrometer to systematically study light quark mesonic states up to masses of around 3.5 Gev/c^2. There are a number of desirable features which make MesonEx particularly suitable for such a study. First, the high luminosity electron beam will provide a high flux of quasi-real virtual photons producing mesons with a relatively high cross sections compared to deep inelastic measurements which will run in parallel. Second, by measuring the scattering plane of the electron the resulting quasi-real photon will be linearly polarized providing an additional handle for studying the production and decay of the mesons. Third, as we can measure all contributing particles the initial and final states are clearly identified providing a clean sample of many reactions for interpretation (which may still be challenging).

XVIth International Conference on Hadron Spectroscopy
AIP Conf. Proc. 1735, 070003-1–070003-7; doi: 10.1063/1.4949451
Published by AIP Publishing. 978-0-7354-1389-4/$30.00

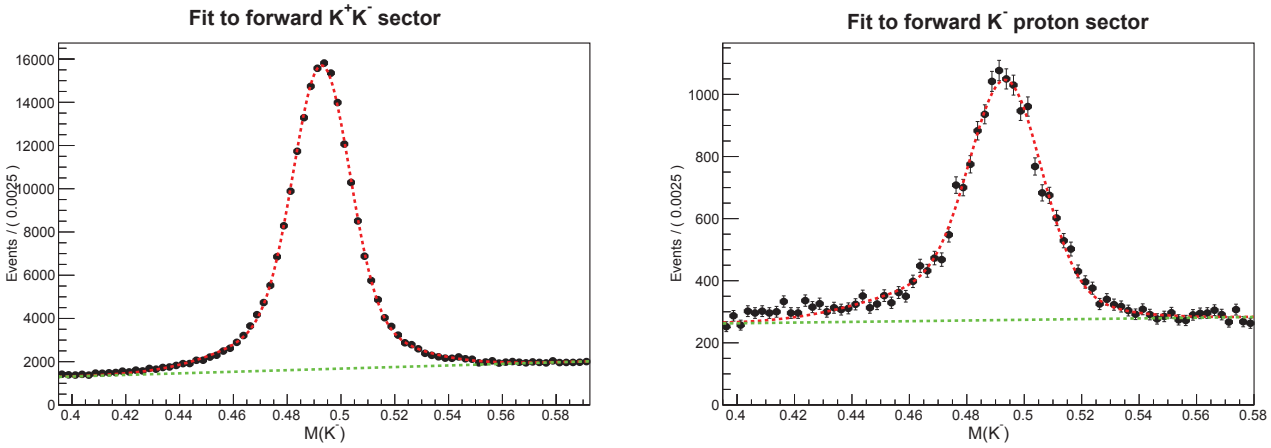

FIGURE 1. Two fits to the reconstructed K^- mass (calculated from beam, target, K^+ and proton four-vectors) used to calculate sWeights for the K^+K^-proton Longitudinal Phase Space analysis. The left plot are for events in the forward K^+ and K^- region and the right plot for the forward K^- proton region. The red line shows the total fit while the green is a polynomial giving the background contribution.

HASPECT

As alluded to in the previous section having a clean event sample for a number of reactions is highly desirable for interpreting the underlying states and processes. However from a data analysis perspective the challenge is only just starting at this point. It is crucial that the most sophisticated theoretical models are used to directly interrogate the high statistics experimental data to provide the most reliable interpretation. To help facilitate this combination a direct collaboration of experimentalists from CLAS12, and theorists from JPAC [1] has been working to prepare for the upcoming data. The aim of the HASPECT (HAdron SPEctroscopy CenTer) project [2] is to address the need for more elaborate tools in amplitude analysis of high statistics experimental datasets, and the MesonEx experiment in particular. This is part of a global effort in developing tools for spectroscopy analysis [3].

Currently the focus is on handling the data provided from the original CLAS detector, isolating the final state of interest, investigating different contributing processes, such as meson or baryon production, implementing amplitudes supplied by JPAC and performing fits to the data using IU AmpTools [4]. This article will focus on two specific aspects of this: investigating processes using van Hove plots; and fitting with AmpTools and Nested Sampling.

Data Handling

For analyzing MesonEx data we have been developing a software framework based on CERN ROOT libraries. This is based on the TSelector class in conjunction with the parallel processing facility PROOF. Analysis proceeds as a series of steps the output of each being a histogram or a ROOT tree. In principal the new software is general and can operate on any input tree of data. Additional classes have been constructed to perform signal and background seperation. Two methods are currently employed: Weights [5] and Q-value [6]. Weights is well established in high energy experiments and the RooStats project provides an algorithm for calculating these based on RooFit probability density functions (see Fig. 1 for an example). This technique relies on the variable one would like to analyze to being uncorrelated with the variable one fits to discriminate signal and background. Then it works as a sophisticated side-band subtraction in that it does not require samples of signal and background events that are completely isolated. Q-value is a technique that has been developed for analysis of CLAS data and is featured in several publications. It is based on calculating a probability that an event is signal or background based on a fit to a discriminating variable only including the nearest few hundred events in kinematic space.

This article will now focus on the development of Longitudinal Phase Space analysis and Nested Sampling for maximum likelihood fits.

Longitudinal Phase Space

Longitudinal Phase Space analysis for reactions of the type $A+B \rightarrow C_1+C_2+...+C_N$ is a method to reduce the number of dimensions that need be considered, simplifying the separation of different contributing processes. In general, for a reaction of N particles in the final state we have 3N-4 independent dimensions to consider when we use energy and momentum conservation. However, Van Hove [7] demonstrated that at high energy and low transverse momenta the number of useful dimensions can be reduced to N-2. This assumes that the longitudinal momentum component of the final state particles carries most of the useful information. Away from the high energy limit a further variable is required. For the case, N=3, the number of dimensions is just two and Van Hove suggested a variable ω which accounts for the relative strength and direction of the longitudinal momentum of the three particles. In terms of the longitudinal momentum component of the final state particles, p_{Li}, the polar coordinates of the longitudinal phase space plot are given by radial coordinate $\sqrt{\frac{3}{2}}P_L$ and angular ω:

$$\omega_0 = \sin^{-1}\sqrt{\frac{3}{2}}\frac{p_{L1}}{P_L} \quad \omega = \omega_0 \quad for \quad \omega_0 < \frac{\pi}{2} \quad and \quad \omega = \pi - \omega_0 \quad for \quad \omega_0 > \frac{\pi}{2}$$

$$P_L = (\sum_{i=1}^{N} p_{Li}^2)^{\frac{1}{2}}$$

K^+K^-p Final State

The CLAS collaboration has previously published detailed measurements of the $\gamma p \rightarrow \phi p$ reaction including $\phi \rightarrow K^+K^-$ [8]. However many other reactions can contribute to the same final state and, as in this case, there are quite narrow states involved. It provides a nice illustration for investigating the applicability of the Van Hove method. Figure 2 shows a preliminary analysis of the Van Hove plot defined by ω and P_L for this final state. The majority of events cluster in the segment corresponding to a forward (positive longitudinal momentum in CM) K^+ and K^- with the proton recoiling backward. This is the signature for a meson produced in the t-channel, for example ϕ production. In addition there is noticeable structure in the top segment consisting of a forward K^+ and backward K^-, p. This corresponds to a hyperon produced in association with a forward K^+ which could be from kaon exchange or the decay of an s-channel nucleon resonance. The latter could contribute equally to the inverse configuration where the K^+ is emitted backwards.

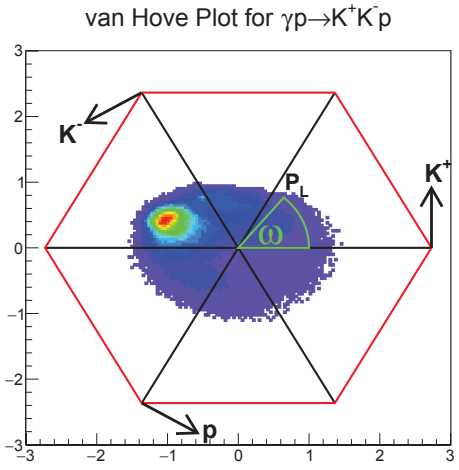

FIGURE 2. A Van Hove plot for the preliminary analysis of the K^+K^-p final state. The three axes labeled K^+, K^- and p, indicate the sign of the relevant particle momentum in the CM frame, with the particle having greater momentum the further it is from the axis.

To learn more about the actual reactions contributing to the acceptance corrected Dalitz plots for events in each segment are shown in Fig. 3. In addition these plots have been background subtracted using the sWeights technique with sample fits shown in Fig. 1.

The t-channel meson segment with forward K^+K^- is dominated by ϕ production at around $M(KK) = 1.02(GeV/c^2)$. The forward K^+ region is mostly $\Lambda(1520)$ production with a threshold enhancement perhaps relating to the $\Lambda(1405)$ also evident. On the other hand the backward K^+ (forward K^-p) region, while containing a lesser sample of $\Lambda(1520)$, shows clear additional hyperons at 1700 and 1800 (MeV/c^2). This suggests a forward production mechanism for the 1700 state as if there is no strong signal for it in any other sector. The 1800 (MeV/c^2) structure also appears in the two sectors where the K^+ and proton are paired, particularly when they travel in the forward direction. When they travel backward this state appears alongside what looks like meson resonances at around 1300 ($f_2(1270)$ or $a_2(1320)$) and 1520 (MeV/c^2) ($f_2'(1270)$). As there are not expected to be any K^+p resonances and the masses plotted are for the other two particle combinations we would not at first expect structure in these two sectors. The reason there is structure is pure kinematics. Heavier particles produced in the original production reaction will travel in the CM frame with a relatively slow speed. When they decay their reaction products can have a greater speed and can therefore switch to a different sector when their decay angle is backward relative to its heavy parent momentum.

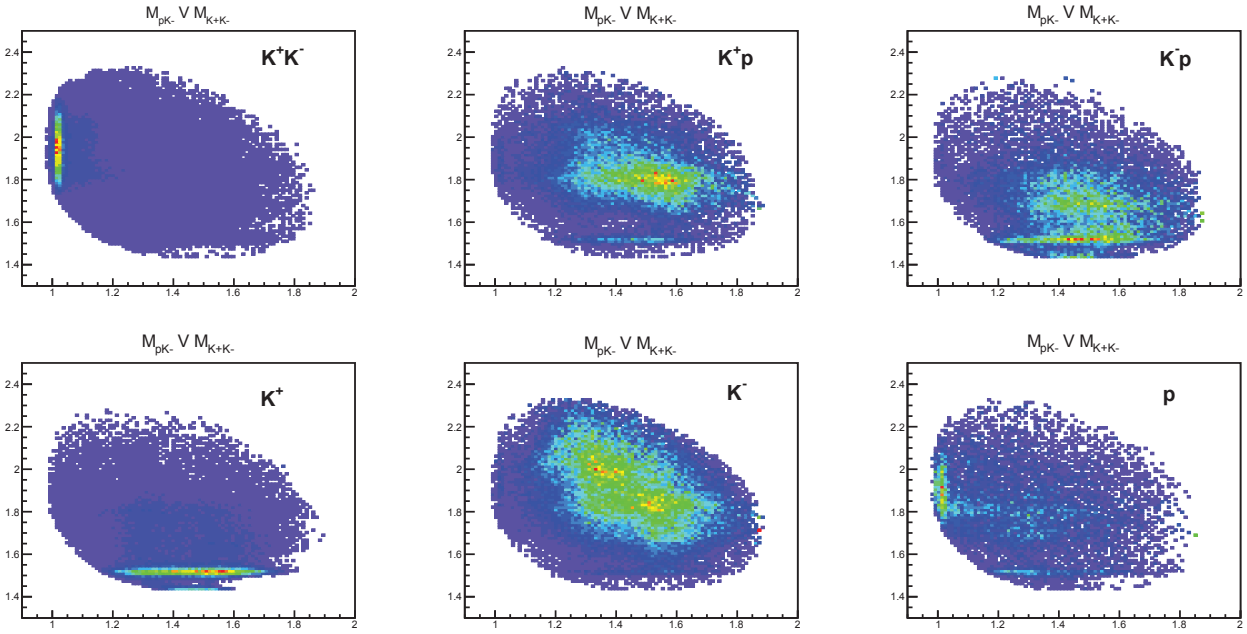

FIGURE 3. Preliminary Dalitz plots with acceptance correction and sWeights background subtraction, for the K^+K^-p final state split into the six segments of the van Hove plot. The axes show the mass in GeV/c^2 for the combined K^+K^- (x) and K^-p (y). The particles given in the top right of each plot indicate which were traveling forward in the CM frame.

Likelihood Analysis

The key part of a meson spectroscopy analysis is finally fitting a model to the signal that has been carefully extracted from the experimental data. Traditionally this has involved performing a χ^2 minimization or by maximizing the likelihood, both using the Minuit package based on a gradient descent to a stationary point in χ^2 or likelihood space. This approach has a number of drawbacks when faced with the complex amplitudes required to fit hadron spectroscopy data which can in principal be remedied through the more robust Bayesian inference techniques [9]. As amplitudes must be squared to fit intensities there can be an intrinsic ambiguity in the correct fit parameters. Mathematically it is possible to resolve ambiguities by, for example, measuring a full set of polarization observables; however, it is now realized that in practice this is not always the case due to finite uncertainties and resolution effects [10, 11].

Another issue with the traditional approach is how to handle local minima and therefore how to choose initial values of fit parameters. Currently there is no rigorous method for doing this and the tendency is to perform an arbitrary number of fits with random initial parameters. Monte-Carlo sampling techniques provide a natural solution for this as they sample the complete parameter space in a well defined manner and provide the full set of possible maxima in the Likelihood space. Finally, Bayesian techniques such as Nested Sampling [12] provide a quantified goodness of fit estimate in the Bayesian evidence. This allows objective comparisons of how well different models fit the data and automatically incorporates Occam's Razor for penalizing models with large numbers of parameters. This is not easily achievable from a maximum likelihood alone. This could prove particularly useful in meson spectroscopy for determining a sufficient set of waves with which to fit the data.

Recently an efficient multimodal Nested Sampling algorithm, MultiNest, was devized by Feroz and Hobson [13]. To investigate whether such methods are suitable for meson spectroscopy we have recently incorporated this likelihood analysis with the Indiana University AmpTools software [4]. AmpTools allows the calculation of a likelihood from the intensity given by user-defined amplitudes. It then uses the Minuit package to find the parameters which yield the maximum likelihood value.

Nested Sampling

The Nested Sampling algorithm starts from Bayes Theorem:

$$L(\theta) \times \pi(\theta) d\theta = Z \times p(\theta) d\theta, \quad (1)$$

$$Likelihood \times Prior = Evidence \times Posterior. \quad (2)$$

where θ is a set of parameters we wish to determine by fitting a model to some data. The Likelihood is the probability that the data is described by the model and parameters θ; the Prior reflects our current knowledge of the θ and may just be some physical bounds, but could also be constraints from previous measurements or theory; the posterior is what we would like to know, the probability of particular parameter values given the data and model; while the Evidence is the Likelihood integrated over the Prior of the parameters, it is also know as the marginal likelihood and can be used to compare different model assumptions through the ratios of evidence (Bayes factors). This latter point can be particularly useful for fitting particular wave sets to spectroscopy data as adding in additional waves that do not significantly increase the likelihood results in large areas in parameter space of low likelihood contributing to and lowering the Evidence. The focus of Nested Sampling compared to other Bayesian Monte-Carlo methods is that it explicitly calculates the Evidence with the Posterior being a by-product. Without going into additional detail Nested Sampling results in a value for the Evidence and a Posterior sample of points containing the parameter values and probablity for each. The distribution of the points will be clustered around regions of high likelihood, i.e. where the parameter values are most probable.

Dalitz Plot Fit

IU AmpTools comes with some beginner tutorials. To test MultiNest for amplitude parameter parameterization we interfaced its maximum likelihood algorithm with the standard "Dalitz" tutorial. This mimics the decay of a resonance X, mass $3(Gev/c^2)$ to three lighter states of mass $0.2(GeV/c^2)$ (P_1, P_2, P_3). Included in the decay are two Breit-Wigner isobar decay amplitudes in the P_1P_2 and P_1P_3 channels with masses 1 and 1.5 GeV/c^2, respectively. The intensity function to be fitted is the coherent sum of these two amplitudes:

$$I(M_{12}, M13) = (V_{12}BW(M_{12}) + V_{13}BW(M_{13}))^2 \quad (3)$$

where $V_{12,13}$ are the complex production amplitudes which we hope to determine from the fit. In the standard tutorial events are first generated for equal production amplitudes. An event-by-event extended log-likelihood fit is then performed using a Minuit minimizer. The values returned are $V_{12}(re) = 30.98 \pm 0.48$, $V_{13}(re) = 30.98 \pm 0.48$ and $V_{12}(im) = -3.01 \pm 1.85$.

We ran the same fit now using the MultiNest sampling of the likelihood. Figure 4 show the final results for the posterior distributions (top) and the "live points" at fit termination (bottom). When the fit terminates the live points are those with the highest sampled likelihood and so cluster round the determined parameter values. From these distributions we see that there are actually two equally probable solutions. MultiNest actually provides a clustering

algorithm for distinguishing the two modes and returns the mean and rms of each cluster (alternatively it can return the maximum likelihood or maximum-a-priori values for each mode). The MultiNest results:

$$1 \quad V_{12}(re) = 30.96 \pm 0.34 \quad V_{12}(im) = 3.03 \pm 1.33 \quad V_{13}(re) = 30.64 \pm 0.32,$$

$$2 \quad V_{12}(re) = -30.96 \pm 0.34 \quad V_{12}(im) = 2.94 \pm 1.30 \quad V_{13}(re) = -30.64 \pm 0.32.$$

The results from MultiNest are consistent with those from Minuit but it is clear more information is provided by the likelihood over the full amplitude space.

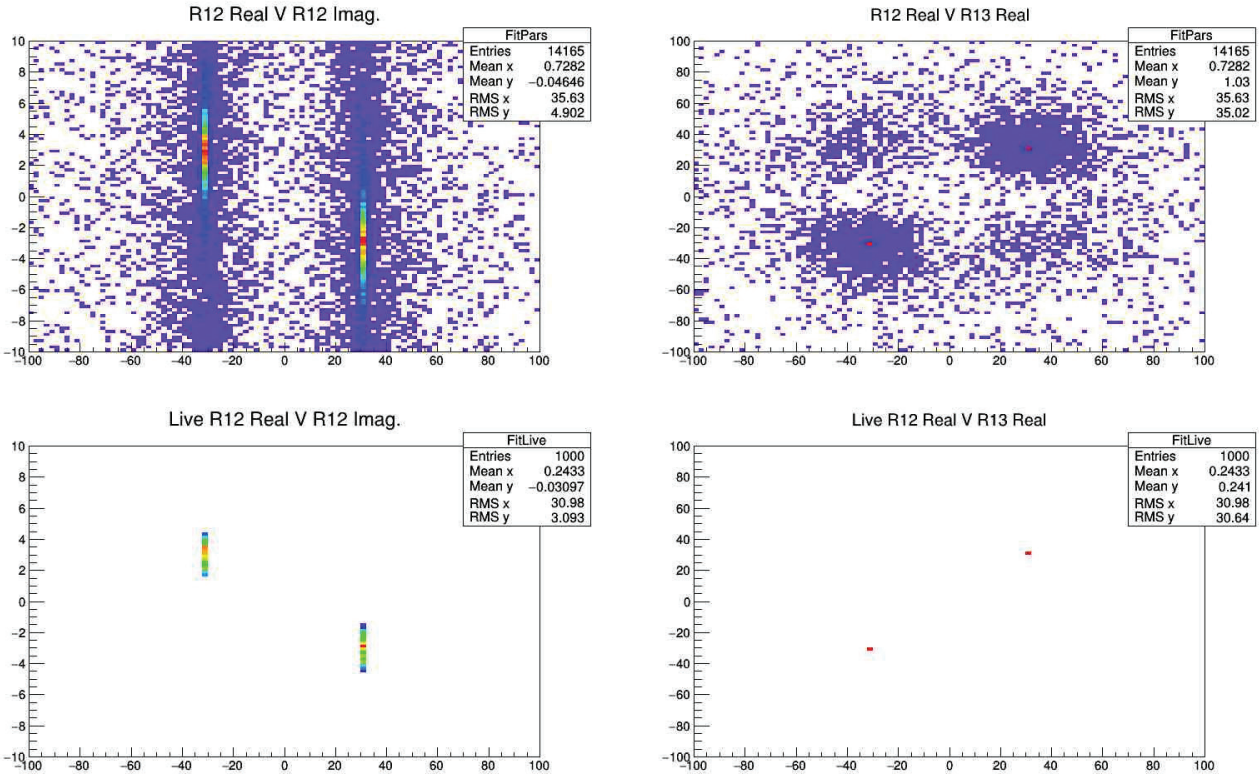

FIGURE 4. MultiNest samples for the production amplitudes projected on two dimensions. Left is the real versus imaginery part of V_{12} and right is the real part of V_{12} versus V_{13}. The top plots show the overall posterior distributions, while the bottom plots show the 1000 points with the greatest likelihood. Two solutions are clearly identified, while there are also signs of local maxima with real parts of opposite signs.

Conclusions

The upgraded CEBAF accelerator and CLAS12 detector system will soon provide data with high statistics for electro and photo-induced reactions. To prepare for analysis of the data the HASPECT collaboration in conjunction with JPAC have been investigating techniques that may be applicable to analyze meson spectroscopy reactions. Two such methods which have been described here are Longitudinal Phase Space analysis and Nested Sampling for maximum likelihood determination. We find that both have the potential to enhance our understanding of the contributing reactions.

ACKNOWLEDGMENTS

The author acknowledges the contribution of Viktor Nodgren who implemented the MultiNest algorithm within AmpTools as part of an undergraduate Summer project at the University of Glasgow.

REFERENCES

[1] Joint Physics Analysis Center http://www.indiana.edu/ jpac/, .
[2] E. Santopinto, Journal of Physics: Conference Series **527**, p. 012028 (2014).
[3] M. Battaglieri, Acta Physica Polonica B **46**, p. 257 (2015), arXiv: 1412.6393.
[4] AmpTools http://sourceforge.net/projects/amptools/files/, .
[5] M. Pivk and F. R. L. Diberder, Nuclear Instruments and Methods in Physics Research Section A: Accelerators, Spectrometers, Detectors and Associated Equipment **555**, 356–369December (2005), arXiv: physics/0402083.
[6] M. Williams, M. Bellis, and C. A. Meyer, Journal of Instrumentation **4**, P10003–P10003October (2009), arXiv: 0809.2548.
[7] L. Van Hove, Physics Letters B **28**, 429–431January (1969).
[8] B. Dey, Phys. Rev. C **89**, p. 055208May (2014).
[9] L. McCandless, Statist. Med. **28**, 3467–3468November (2009).
[10] L. Tiator, arXiv:1211.3927 [nucl-th] November (2012), arXiv: 1211.3927.
[11] J. Nys, T. Vrancx, and J. Ryckebusch, J. Phys. G: Nucl. Part. Phys. **42**, p. 034016 (2015).
[12] J. Skilling, Bayesian Anal. **1**, 833–859December (2006).
[13] F. Feroz and M. P. Hobson, Monthly Notices of the Royal Astronomical Society **384**, 449–463January (2008), arXiv: 0704.3704.